

# High-efficiency Steady-State CEST using continuous spiral acquisition.

Johannes Hammacher<sup>1</sup>, Christoph Kolbitsch<sup>1</sup>, Patrick Schünke<sup>1</sup>

<sup>1</sup>Physikalisch-Technische Bundesanstalt, Braunschweig and Berlin, Germany

**INTRODUCTION:** CEST MRI is poised to become a vital part in clinical diagnostics due to its specificity and versatility<sup>1</sup>. However, challenges remain that hinder its wider adoption such as long scan times, poor image quality and high variability due to motion<sup>2</sup>. Compared to traditional CEST sequences, steady-state CEST (ssCEST) sequences have demonstrated the potential to markedly reduce data acquisition times<sup>3</sup>. Importantly, these enable to acquire data continuously and to utilize advanced image readouts<sup>4</sup>. Previous work has shown that radial trajectories can be used within continuous ssCEST sequences<sup>5</sup>. Here, we propose to improve the k-space coverage efficiency and robustness of ssCEST sequences using spiral trajectories<sup>6</sup>. In addition, we optimized the saturation settings to further reduce scan times while maintaining comparable image quality and CEST effect sizes.

**METHODS:** All sequences (**A.1-A.3**) were implemented using the open-source framework Pulseseq<sup>7</sup>. Each sequence entailed 69 frequency offsets and the same number of acquired k-space points per offset resulting in 200 radial spokes (256 samples each) and 128 spirals (400 samples, each) that were subsequently rotated by the golden angle (107°), respectively. Gaussian-shaped RF pulses with B1 = 2  $\mu$ T were used in all cases. Acquisition parameters were: 256 mm FOV, 1 mm in-plane resolution, 10 ms TR, 15° flip angle. For *in vitro* scans, APTw-phantoms containing egg-white were used<sup>8</sup>. Four radial and four spiral sequences were tested on the phantom with differing saturation pulse durations (25 ms, 50 ms, 75 ms, 100 ms) before every readout. A conventional cartesian CEST sequence with a preceding saturation block (25x100 ms, DC 50%) was used for comparison. Post-processing was done using open-source in-house developed reconstruction frameworks.

**RESULTS:** Results of the phantom experiments are shown in figure **B**. Z-Spectra and asymmetry plots were generated from regions of interest (ROIs). The radial and spiral ssCEST sequences exhibited similar APT effect sizes compared to the conventional CEST sequence. A reduction of the saturation time led to a reduction of the acquisition times (**Fig. C.2**), but down to 50 ms to no essential reduction of the APT effect sizes for both ssCEST sequences (**Fig. C.1**). For the investigated cases, the spiral sequence is about 50% faster compared to the radial one (**Fig. C.2**). For the *in vivo* measurements, the optimized saturation time of 50 ms was used. Figure **D.1-D.3** shows that the image quality within the brain is comparable between all three investigated sequences yielding the same APT effect sizes, while the acquisition time of the spiral ssCEST sequence is shorter compared to the other sequences.

**DISCUSSION:** In addition to the benefit of faster acquisition times, the proposed spiral ssCEST sequence has a great potential for more complex imaging settings, such as liver. In general, radial and spiral trajectories are inherently more robust to bulk-motion artifacts due to repeated sampling near the center of the k-space. Moreover, these acquisitions can be used with higher undersampling factors. In conjunction with advanced reconstruction methods, including AI, they have the potential to accelerate CEST measurements even more. Finally, 3D acquisitions are possible as well, leaning onto previously published 3D stack-of-stars (stack-of-spirals in this case) sequences<sup>9</sup>.

**CONCLUSION:** Spiral readout trajectories have the potential to significantly accelerate CEST sequences. Our results already show considerable reductions in total acquisition times while maintaining high image quality. Moreover, they pose as a starting point for further optimizations that will enable faster, more efficient CEST measurements throughout the body.

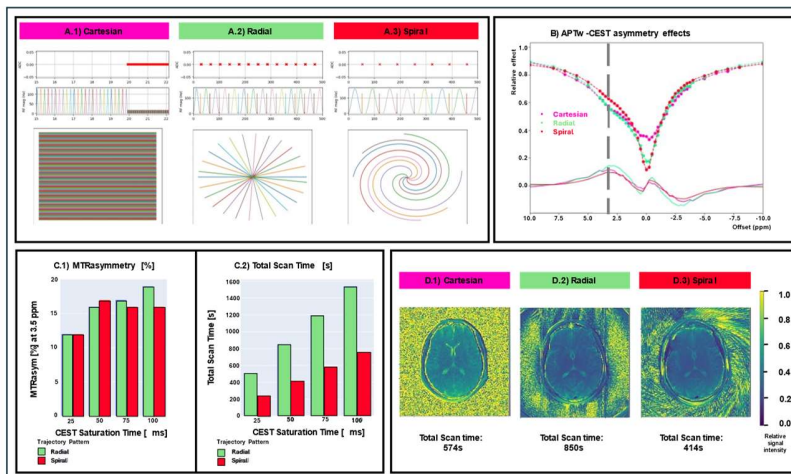


**Figure: A.1-A.3)** Acquisition trajectories—cartesian centric-out, radial and spiral. Pulse-sequence diagrams exemplify ADC use and RF pulse-train respectively. Bottom panels show visualizations of the according k-space acquisition pattern. **B)** Exemplary results for egg-white phantom scans using the different readouts. **C.1-C.2)** Quantifications regarding total acquisition time, as well as MTR-asymmetry at 3.5 ppm (%) for four saturation times (25, 50, 75, 100 ms), respectively. **D.1-D.3)** Reconstructed images from volunteer brain scans. Colors indicate normalized signal intensity. Individual images show volunteer brain at 3.5 ppm offset from water. Notably, spiral acquisitions show comparable image quality to radial readouts, despite being 50% faster.

## REFERENCES:

1. Jones, K. M., Pollard, A. C. & Pagel, M. D. Clinical applications of chemical exchange saturation transfer (CEST) MRI. *J. Magn. Reson. Imaging* **47**, 11–27 (2018).
2. Van Zijl, P. C. M. & Yadav, N. N. Chemical exchange saturation transfer (CEST): What is in a name and what isn't? *Magn. Reson. Med.* **65**, 927–948 (2011).
3. Kim, B., So, S. & Park, H. Optimization of steady-state pulsed CEST imaging for amide proton transfer at 3T MRI. *Magn. Reson. Med.* **81**, 3616–3627 (2019).
4. Han, P. *et al.* Whole-brain steady-state CEST at 3 T using MR Multitasking. *Magn. Reson. Med.* **87**, 2363–2371 (2022).
5. Ran Sui; Lin Chen; Yuguo Li; Jianpan Huang; Kannie W. Y. Chan; Xiang Xu; Peter C. M. Zijl; Jiadi Xu. Whole-brain amide CEST imaging at 3T with a steady-state radial MRI acquisition. *Magn. Reson. Med.* (2021).
6. Heidemann, R. M. *et al.* Direct parallel image reconstructions for spiral trajectories using GRAPPA. *Magn. Reson. Med.* **56**, 317–326 (2006).
7. Layton, K. J. *et al.* Pulseseq: A rapid and hardware-independent pulse sequence prototyping framework. *Magn. Reson. Med.* **77**, 1544–1552 (2017).
8. Zhou, J., Yan, K. & Zhu, H. A Simple Model for Understanding the Origin of the Amide Proton Transfer MRI Signal in Tissue. *Appl. Magn. Reson.* **42**, 393–402 (2012).
9. Han, P. *et al.* Free-breathing 3D CEST MRI of human liver at 3.0 T. *Magn. Reson. Med.* **89**, 738–745 (2023).